Nanoscale

COMMUNICATION

View Article Online
View Journal | View Issue

Cite this: *Nanoscale*, 2017, **9**, 1443

Received 22nd November 2016,
Accepted 29th December 2016

DOI: 10.1039/c6nr09074e

www.rsc.org/nanoscale

A universal mechanism of the planar boron rotors B_{11}^-, B_{13}^+, B_{15}^+, and B_{19}^-: inner wheels rotating in pseudo-rotating outer bearings†

Yonggang Yang,*[a,b] Dongming Jia,[a] Ying-Jin Wang,[c] Hua-Jin Zhai,*[c] Yuan Man[a,b] and Si-Dian Li*[c]

Planar boron clusters B_{11}^-, B_{13}^+, B_{15}^+, and B_{19}^- have been introduced recently as molecular Wankel motors or tank treads. Here we present a universal mechanism for these dynamically fluxional clusters; that is, they are molecular rotors with inner wheels that rotate almost freely in pseudo-rotating outer bearings, analogous to rotating molecules trapped in pseudo-rotating cages. This mechanism has significant quantum mechanical consequences: the global-minimum structures of the clusters have C_{2v} symmetry, whereas the wheels rotating in pseudo-rotating bearings generate rosette-type shapes with D_{9h}, D_{10h}, D_{11h}, and D_{13h} symmetries. The related rotational/pseudo-rotational energies appear with characteristic band structures, effecting the dynamics.

Molecular rotors are a hot topic in chemistry and neighboring disciplines, with fascinating applications to systems in the gas phase,[1–5] in solution,[1,6–8] in crystals,[1,9] on surfaces,[1–3,10–13] and in the biological environment.[14] In fact, molecular rotors may serve to perform different molecular tasks in a sequential manner, with the sequence being controlled by the directionality of a rotary cycle.[8,14]

The purpose of this Communication is to present a new type of mechanism, that is, molecular rotors with inner wheels rotating almost freely in pseudo-rotating outer bearings, with applications to a series of planar boron clusters: B_{11}^-,[15] B_{13}^+,[16–18] B_{15}^+,[19] and B_{19}^-.[20,21] The mechanism is analogous to rotating molecules in pseudo-rotating cages,[22] as demonstrated for weakly interacting host–guest systems such as molecules isolated in rare gas matrices,[22] or in quantum crystals (*para*-hydrogen).[23,24] Previously these boron clusters were presented as molecular Wankel motors or tank treads, with low energy barriers for the intramolecular rotations of the wheel, but without the recognition of the pseudo-rotational motion of the bearing.[15–21] The given names suggest applications in molecular machines, but this still awaits further experimental verification. In any case, at first, the low energy barriers of the covalently bonded planar boron rotors came as a surprise, but then this common phenomenon was unraveled in detail.[15–21] Essentially, it is linked to their aromaticity due to delocalized (π and σ) bonding. These discoveries contributed to the exciting development of the field of the boron clusters ranging from planar clusters,[25–29] borospherenes,[29–31] to borophenes,[29,32,33] comparable to the milestone advances in all-carbon systems.[5,34–36]

Our proposed new mechanism will be explained in detail using the planar rotor B_{11}^- as an example, with fundamental quantum mechanical consequences for molecular structure, symmetry, energetics, and dynamics. Selective analogous results will then be presented for larger molecular rotors: B_{13}^+, B_{15}^+, and B_{19}^-. From the outset, it is worth mentioning that interpretations of the results may depend on different frames of observation. For example, from the perspective of the molecular wheel, the outer bearing appears as if it moves around the wheel.[17,19–21] In contrast, in the laboratory frame, the light compact inner wheel rotates in one direction much faster than the opposite rotation of the heavy outer bearing (see the ESI† for the details).

The derivation of the mechanism of boron rotors B_{11}^-, B_{13}^+, B_{15}^+, and B_{19}^- is based on previous results of photoelectron spectra, quantum chemistry calculations of the structures of the global minima (GM) and transition states (TS) and their barrier heights, and molecular dynamics simulations.[15–21] The relevant facts are as follows: the total number of boron nuclei, N_t = 11, 13, 15, 19, consist of the numbers for the wheels, N_w = 2, 3, 4, 6, plus those for the bearings, N_b = 9, 10, 11, 13, respectively. Furthermore, N_w may be written as $N_w = N_s + N_c$, where N_s = 2, 3, 4, 5 are the number of boron nuclei that form the shapes of the wheels, and N_c = 0, 0, 0, 1 are the numbers

[a]*State Key Laboratory of Quantum Optics and Quantum Optics Devices, Institute of Laser Spectroscopy, Shanxi University, Taiyuan 030006, China. E-mail: ygyang@sxu.edu.cn*
[b]*Collaborative Innovation Center of Extreme Optics, Shanxi University, Taiyuan 030006, China*
[c]*Nanocluster Laboratory, Institute of Molecular Science, Shanxi University, Taiyuan 030006, China. E-mail: hj.zhai@sxu.edu.cn, lisidian@sxu.edu.cn*

†Electronic supplementary information (ESI) available: Quantum chemistry calculations and reaction paths; the effective moment of inertia; quantum mechanical calculations; and quantum dynamics simulation. See DOI: 10.1039/c6nr09074e

of central boron nuclei: B_{19}^- is the only boron rotor with a nucleus sitting at the wheel's axle.[20,21] The wheels and bearings are coplanar, and the rotations are about the axes perpendicular to the molecular x–y planes, intersecting at the molecular centers of mass (c.o.m). Clusters B_{11}^-, B_{13}^+, B_{15}^+, and B_{19}^- have $N_m = N_s \cdot N_b = 18, 30, 44, 65$ equivalent planar global-minimum structures GM_i, $i = 1, 2, ..., N_m$, which may be listed in a cyclic manner such that $GM_{N_{m+1}} = GM_1$. All GM_i structures have C_{2v} symmetry. The GM_i's are separated from each other by N_m equivalent transition states $TS_{i,i+1}$'s. The $TS_{i,i+1}$ have very low energy barriers $V_b \approx 0.64, 0.30, 1.30, 0.02$ kcal mol^{-1}, respectively, facilitating nearly free rotation of the molecular wheels in their bearings. The $TS_{i,i+1}$'s are also planar, again with C_{2v} symmetries. One rotational cycle of the molecular wheels with respect to their bearings corresponds to the motion along the cyclic reaction paths (CRPs) *via* the cyclic sequence of GM_i's. These paths are called "rotational/pseudo-rotational CRPs" (rpr-CRP). The in-plane lowest-frequency normal modes of all GM_i structures and the imaginary-frequency normal modes for crossing $TS_{i,i+1}$ correlate with motions along the rpr-CRP.

Let us now use these results[15–21] to derive the new mechanism of rotating wheels in pseudo-rotating bearings, exemplarily for the B_{11}^- rotor.[15] During this course, we shall also present the corresponding general expressions (in brackets), which are valid for all planar boron rotors. For simplicity, we consider boron clusters consisting of pure ^{11}B isotope (with mass $m_B = 11.01$ u). One of the global-minimum structures (for convenience, we choose GM_{18}, or in general GM_{N_m}) and a neighboring transition state ($TS_{18,1}$, or in general $TS_{N_m,1}$) are shown in Fig. 1a and b, respectively. The orientation of the lever-type wheel with respect to the horizontal x-axis is specified by angle φ. The in-plane lowest-frequency normal mode of GM_{18} and the imaginary-frequency normal mode of $TS_{18,1}$ are illustrated by arrows in Fig. 1a and b, respectively.

Before explaining the mechanism, it is helpful to consider the in-plane molecular rotations first. Exemplarily, Fig. 1c shows the effect of rotating GM_{18} by $k \cdot 40°$, $k = 0, 1, 5$, (in general: by multiples of $\varphi_{N_b} = 360°/N_b$). We observe two consequences owing to the fact that, quantum mechanically, the sets of boron nuclei are indistinguishable. Firstly, the molecular structure does not change if the central wheel is back-rotated by 180° (in general: by multiples of $360°/N_s$). Thus the molecular rotations by 200, 240, 280, and 320° are equivalent to rotations of the wheel by 20, 60, 100, and 140°, accompanied with rotations of the bearings by 200, 240, 280, and 320°. Second, Fig. 1c shows that the structures generated by rotations of the bearing can alternatively be generated by motions of the individual boron nuclei of the bearing. It is important that these nuclei move concertedly, very different from the random adjustment of a soup of atoms that surround the wheel. The concerted motions are called pseudo-rotations since they rotate the shapes of the bearings only, without rotating the bearings. Fig. 1e shows the corresponding sequence of nine (in general: N_b) rainbow-color-coded snapshots of the two (in general: N_w) nuclei of the rotating wheel on two semi-circles, in angular steps of 20° (in general: $360°/N_m$) surrounded by nine (in general: N_b) pseudo-rotating nuclei of the bearing, all moving on equivalent periodic orbits; here they are approximately ellipsoidal. The corresponding molecular structures are identified as global-minima GM_1, GM_2, ..., and GM_9

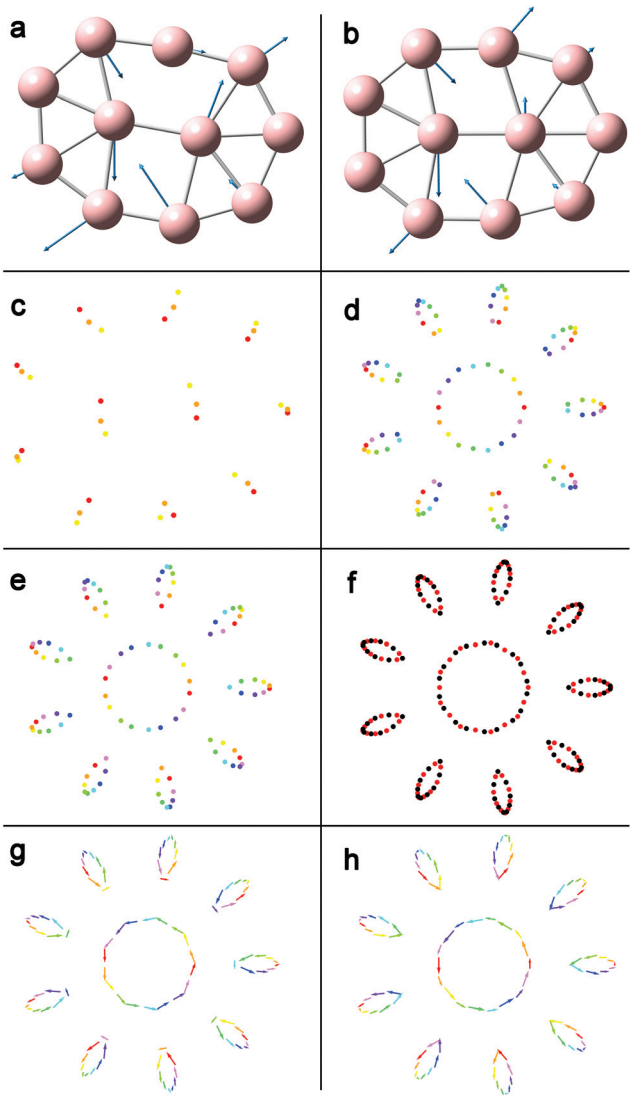

Fig. 1 From the global-minimum structures (GM) and transition states (TS) of the planar boron rotor B_{11}^- to the mechanism of a wheel rotating in a pseudo-rotating bearing. (a and b) Structures of GM (a) and TS (b) with C_{2v} symmetry, in the molecular x–y plane. Arrows indicate the in-plane lowest-frequency (for GM) and the imaginary-frequency (for TS) normal modes. (c, d, and e) Rainbow-color-coded illustration of the snapshots for rotating the GM (e) or TS (d) by 0, 200, 40, 240, 80, 280, 120, 320, and 160°, or (equivalently) for rotating the wheel by 0, 20, ..., 160° and pseudo-rotating the nuclei of the bearing on equivalent periodic orbits with ellipsoidal shapes. Panel (c) shows the first three snapshots in (e) for didactic purpose. (f) Superposition of (e) and (d), with 18 snapshots of alternating structures of GM (black) and TS (red) along the rotational/pseudo-rotational circular reaction path (rpr-CRP). (g and h) Directions for the nuclear motions along the rpr-CRP, illustrated by the corresponding vectors in (a) and (b) for all GM (g) and TS (h) along the rpr-CRP.

(in general: GM_1, ..., and GM_{N_b}). Continuous rotations of the wheel by nine (in general: by $N_b \cdot (N_s - 1)$) additional steps proceed with the second (in general: the second, third, ..., and N_s-th) identical pseudo-rotational cycle(s) of the nuclei of the bearing. One rotational cycle of the wheel is thus accompanied with two (in general: N_s) concerted pseudo-rotational cycles of the nine (in general: N_b) nuclei of the bearing, all on equivalent periodic orbits. Altogether, the rotation of the wheel combined with the concerted pseudo-rotation of the bearing generates the cyclic sequence of all GM_i's along the rpr-CRP.

The above derivation, from considerations of the rotating molecule to the molecular rotor with rotating wheel in its pseudo-rotational bearing, may also be applied to the GM_i's with the attached arrows for the lowest-frequency (ν_{low}) normal mode (Fig. 1a). The result is shown in Fig. 1g. It illustrates the directions for the nuclear motions along the rpr-CRP. Likewise, the derivation may be applied to the transition states, starting from rotations of $TS_{18,1}$ (in general: $TS_{N_m,1}$), without or with arrows for the normal mode with (imaginary) frequency ν_{im} (Fig. 1b), and ending up with a sequence of snapshots of the rotating wheel in pseudo-rotating bearing, at the $TS_{i,i+1}$'s, together with the directions for nuclear motions along the rpr-CRP. The results are shown in Fig. 1d and h, respectively, analogous to Fig. 1e and g for GM_1, GM_2, ... Fig. 1f shows a superposition of Fig. 1e and d, demonstrating the alternating sequence of snapshots for the structures of GM_i and $TS_{i,i+1}$ along the rpr-CRP.

Having established the mechanism of the molecular rotor with a rotating wheel in its pseudo-rotating bearing, we now deduce some important consequences in terms of structures, symmetries, energetics, and dynamics, starting with the molecular ground state. Quantum mechanically, these properties are represented by wave-functions, which are obtained as solutions of the Schrödinger equations, depending on the potential energies $V(\varphi)$ along φ (representing the rpr-CRP) and on the effective moments of inertia I_{eff} of the rotating molecular wheels in their pseudo-rotating bearings. Accordingly, $V(\varphi)$ has 18 (in general: N_m) equivalent minima for GM_i, separated by 18 (in general: N_m) equivalent transition states $TS_{i,i+1}$. For B_{11}^-, the similarity of the absolute values of the frequencies ν_{low} at GM_i and ν_{im} at $TS_{i,i+1}$ suggests the representative analytical model potential $V(\varphi) = V_b \cdot \cos^2(9\varphi)$, with a barrier height V_b and with a periodic boundary, $V(0) = V(2\pi)$. This is illustrated in Fig. 2. The model is also supported by the fact that all other normal modes of GM_i and $TS_{i,i+1}$ correlate closely with each other, with rather similar frequencies, which means that they are fairly decoupled from motions along the rpr-CRP. Hence our model focuses on the motions of the rotors along their rpr-CRPs, leaving effects of other "spectator" modes for refinements. The force constants at GM_i and at $TS_{i,i+1}$ are related to the frequencies ν_{low} and ν_{im}, and to the effective moment of inertia I_{eff}. The resulting mean value of I_{eff} is $I_{eff,m} = 57.5$ u Å^2, in excellent agreement with the value $I_{eff} = 57.3$ u Å^2 based on the derivation in ref. 22; see the ESI (eqn (S10) and (S15)†).

The wave-function representing the ground state of the boron rotor B_{11}^- is illustrated in Fig. 2, embedded in the potential $V(\varphi)$, at its (zero point) energy, which is also the zero axis for the wave-function in Fig. 2. Accordingly, all 18 potential minima (that is, all the global-minimum structures GM_i) are populated with the same quantum mechanical probability. The equivalent presence of all GM_i structures is illustrated in Fig. 3e, which is adapted from Fig. 1e. Thus, boron rotor B_{11}^- has the quantum mechanical rosette-type structure with D_{9h} symmetry; this is remarkably different from the global-minimum structure with C_{2v} symmetry (compare Fig. 3e and a). Fig. 2 also unravels that significant parts of the wave-function tunnel from the GM_i's to the $TS_{i,i+1}$, which supports the nearly free rotations of the wheel in its pseudo-rotating bearing, even at energies below the barrier.

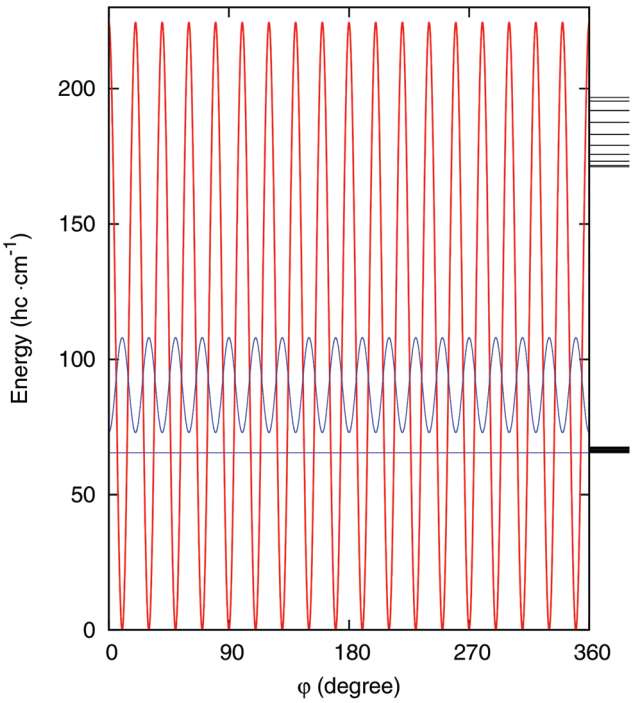

Fig. 2 Wave-function representing the ground state of molecular rotor B_{11}^-, embedded in the potential energy curve (red) for the rotating wheel in pseudo-rotating bearing. The wave-function (blue curve) shows equal populations of all the eighteen equivalent global-minimum structures, which are supported by eighteen equivalent potential wells and separated by eighteen equivalent transition states. The blue horizontal line shows the zero-point energy. Also shown on the right-hand side is the low energy spectrum with two energy bands, a narrower one and a broader one, each with eighteen rotational/pseudo-rotational states.

The spectrum of 36 lowest rotational/pseudo-rotational eigenenergies of B_{11}^- (all below the potential barrier) is also shown in Fig. 2. Apparently, these eigenenergies form bands, indicating signatures for the transition from molecular to condensed state behavior of the boron cluster, B_{11}^-.

During the revision of this manuscript, we became aware of the fascinating very recent (Dec. 2016) publication of M. R. Fagiani *et al.*, which reports the first spectroscopic evidence for the fluxionality of the boron rotor, B_{13}^+.[18] Several

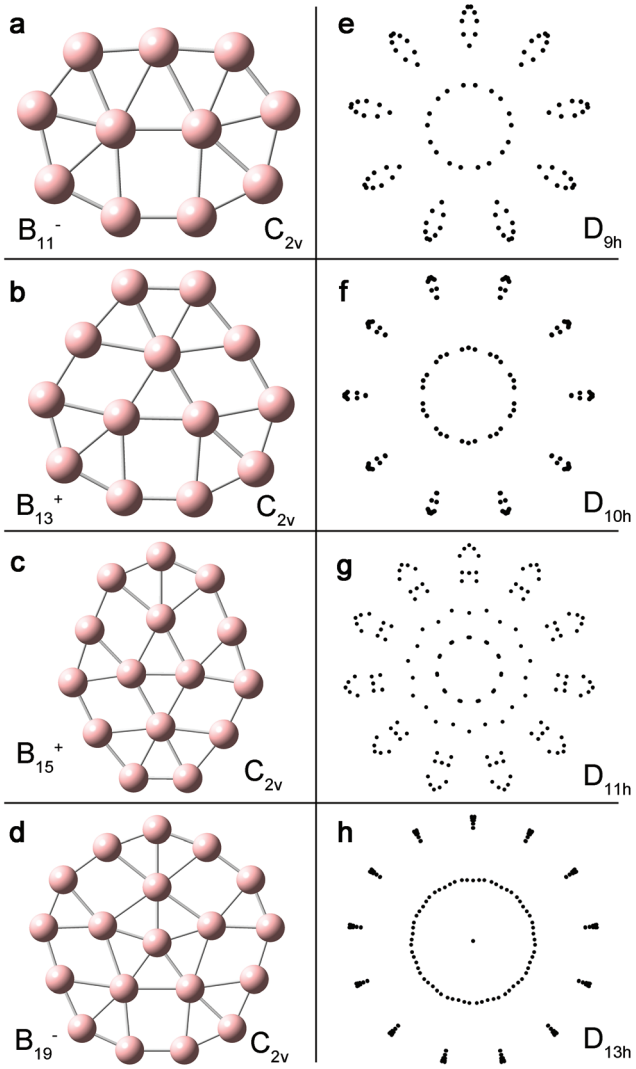

Fig. 3 Comparison of the global-minimum (GM) structures of molecular boron rotors B_{11}^- (a), B_{13}^+ (b), B_{15}^+ (c), and B_{19}^- (d) with C_{2v} symmetry (left), and their rosette-type structures for the ground states of the rotating wheels in pseudo-rotating bearings, with D_{9h} (e), D_{10h} (f), D_{11h} (g), and D_{13h} (h) symmetries, respectively (right). All GM structures in panels (a–d) have their C_{2v} symmetry axis aligned in vertical direction. Dots in panels (e–h) indicate the locations of the maximum (equal) probabilities of observing the boron nuclei.

observations of ref. 18 provide gratifying evidence for our present predictions. We note the following correspondences: an important evidence for the fluxionality of B_{13}^+ in ref. 18 is the significant population of the transition state, which is monitored by a characteristic peak (so-called peak "e") in the cryogenic ion vibrational spectrum; for comparison, this phenomenon is predicted in Fig. 2, even at zero temperature, that is, the transition state is populated by tunneling of the rotational/pseudorotational wave-function. Another intriguing signature of the fluxionality of B_{13}^+ is the line width of the vibrational spectral peaks, which is significantly broader than the spectral linewidth, even at an experimental temperature of 16 K. The present prediction of rotational/pseudo-rotational bands (see Fig. 2) allows the working hypothesis that ref. 18 actually contains the first experimental evidence of such bands, as they should contribute to the width of the vibrational spectra. The correspondences are remarkable and stimulating. Extended applications and developments of the theory for the present universal rotational/pseudo-rotational mechanism of the planar boron rotors are in progress. For example, multidimensional quantum mechanical simulations will provide a detailed understanding of the width of the vibrational spectra and the role of the anharmonic couplings.

Quantum dynamics simulations of the rotating/pseudo-rotating rotor B_{11}^- are demonstrated in Fig. 4, and in Fig. S1 of the ESI;† details of the underlying theory are also presented in the ESI.† For this purpose, we assume that the rotor has been prepared in one of the equivalent global minimum structures, say GM_9, either in its ground state (Fig. 4) or in its first excited rotational/pseudo-rotational state (Fig. S1 of the ESI†). Subsequently, the representative wave-function tunnel from GM_9 through the transition states $TS_{9,10}$ or $TS_{8,9}$ to the neighboring global minimum structures GM_{10} or GM_8, respectively. Note that in quantum mechanics, both rotational directions along φ (anti-clockwise) or along $-\varphi$ (clockwise) proceed with equal probabilities.

Fig. 4 and S1† illustrate the systematic clockwise and anti-clockwise penetrations of the wave-functions from the original position representing GM_9 *via* the sequence of all other GM's in a cyclic manner, until their frontier lobes arrive back to the original structure GM_9, which corresponds to one cycle of the rotational/pseudo-rotational evolution of the rotor. The clockwise and anti-clockwise frontier lobes may interfere destructively or constructively; the latter corresponding to a so-called (partial) revival.[37] Fig. 4 also shows the probability $P_9(t)$ for arriving at the original global minimum structure GM_9 after passing sequentially through all other GM_i's. The time delay from the initial peak $P(t = 0) = 1$ to the first prominent peak of

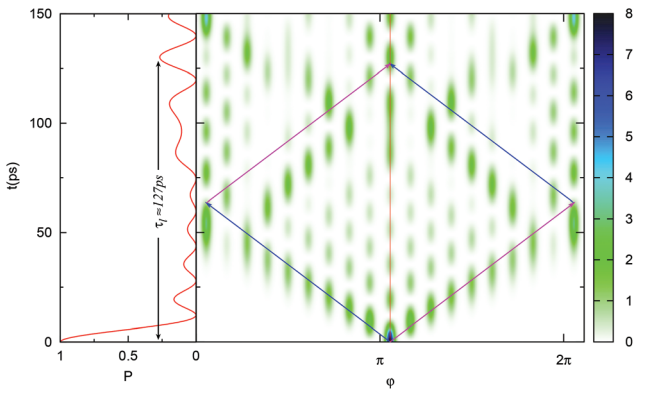

Fig. 4 Time evolution of the population $P(t)$ (left) and of the density (right) of the initial global minimum structure GM_9 of the rotor B_{11}^- prepared in its ground state. The blue and pink arrows should guide the eyes for the cyclic time evolution of the frontier lobes representing the rotating wheel in pseudo-rotating bearing.

$P_9(t = \tau)$ for partial revival yields the corresponding period τ. Quantum dynamics simulations yield $\tau_{lower} \approx 127$ ps (Fig. 4) and $\tau_{upper} = 8$ ps (Fig. S1 of ESI†) for the lower and upper bands, respectively.

Selective results of analogous derivations for larger molecular rotors B_{13}^+, B_{15}^+, and B_{19}^- are shown in Fig. 3, starting from the global-minimum structures GM_{N_m} in panels 3b, 3c, and 3d and ending up with equal quantum mechanical populations of all the $N_m = N_b \cdot N_s$ equivalent structures GM_i of the rotating wheels in their pseudo-rotational bearings, as illustrated in panels 3f, 3g, and 3h, respectively. In general, the boron rotors in the ground states have rosette-type structures, with $D_{N_b h}$ symmetries.

Conclusions

Rotating wheels in pseudo-rotating bearings are thus discovered as a universal mechanism of the planar boron rotors, with important consequences for their structures and symmetries. Additional consequences concerning the occurrence of rotational/pseudo-rotational energy bands and the quantum dynamical rotational/pseudo-rotational periods, in the picosecond time domain, have also been demonstrated for B_{11}^- as an example. Complementary consequences including implications of molecular permutation/inversion symmetries, the role of nuclear spin isomers, and the possibility to ignite and control uni-directionality of the molecular rotors by means of well-designed laser pulses (*cf.* ref. 21), as well as applications to alternative systems such as metal-centered boron rings,[38] will be published separately.

Finally, let us draw a general conclusion by considering the fact that molecular wheels and bearings cannot have perfectly circular shapes due to their atomic structures. For example, the present molecular wheels have double-bladed propeller-type, triangular, rhombic, and pentagonal shapes. It appears as a gift of nature that molecular boron rotors manage to compensate this inevitable deficit of molecular wheels by providing bearings with flexible shapes that can adapt concertedly to the rotating wheels, by pseudo-rotation. This is possibly a unique advantage of boron rotors; for instance, it is quite different from the structurally rigid carbonaceous molecular bearings.[5]

Acknowledgements

We thank ChunMei Liu (Berlin) for encouraging exploratory model simulations. This work received financial support, in part by the Deutsche Forschungsgemeinschaft DFG (project Ma 515/27-1), the Program for Changjiang Scholars and Innovative Research Team (IRT13076), the National Natural Science Foundation of China (Grant No. 11434007, 21573138, 21373130), the talent program of Shanxi, the Natural Science Foundation of Shanxi, China (2014021004), and the State Key Laboratory of Quantum Optics and Quantum Optics Devices (KF201402).

Notes and references

1 G. S. Kottas, L. I. Clarke, D. Horinek and J. Michl, *Chem. Rev.*, 2005, **105**, 1281.
2 B. L. Feringa, *J. Org. Chem.*, 2007, **72**, 6635.
3 M. Yamaki, S. Nakayama, K. Hoki, H. Kono and Y. Fujimura, *Phys. Chem. Chem. Phys.*, 2009, **11**, 1662–1678.
4 G. Pérez-Hernández, A. Pelzer, L. González and T. Seideman, *New J. Phys.*, 2010, **12**, 075007.
5 H. Isobe, K. Nakamura, S. Hitosugi, S. Sato, H. Tokoyama, H. Yamakado, K. Ohno and H. Kono, *Chem. Sci.*, 2015, **6**, 2746–2753.
6 S. P. Fletcher, F. Dumur, M. M. Pollard and B. L. Feringa, *Science*, 2005, **310**, 80–82.
7 J. Wang and B. L. Feringa, *Science*, 2011, **331**, 1429–1432.
8 A. Faulkner, T. van Leeuwen, B. L. Feringa and S. J. Wezenberg, *J. Am. Chem. Soc.*, 2016, **138**, 13597–13603.
9 C. Lemouchi, K. Iliopoulos, L. Zorina, S. Simonov, P. Wzietek, T. Cauchy, A. Rodríguez-Fortea, E. Canadell, J. Kaleta, J. Michl, D. Gindre, M. Chrysos and P. Batail, *J. Am. Chem. Soc.*, 2013, **135**, 9366.
10 D. Horinek and J. Michl, *J. Am. Chem. Soc.*, 2003, **125**, 11900.
11 D. Horinek and J. Michl, *Proc. Natl. Acad. Sci. U. S. A.*, 2005, **102**, 14175.
12 C.-A. Palma, J. Björk, F. Rao, D. Kühne, F. Klappenberger and J. V. Barth, *Nano Lett.*, 2014, **14**, 4461–4468.
13 J. Kaleta, E. Kaletová, I. Císařová, S. J. Teat and J. Michl, *J. Org. Chem.*, 2015, **80**, 10134.
14 A. B. Kolomeisky, *Motor Proteins and Molecular Motors*, CRC Press, Boca Raton, 2015.
15 Y.-J. Wang, X.-Y. Zhao, Q. Chen, H.-J. Zhai and S.-D. Li, *Nanoscale*, 2015, **7**, 16054–16060; S. Jalife, L. Liu, S. Pan, J. L. Cabellos, E. Osorio, C. Lu, T. Heine, K. J. Donald and G. Merino, *Nanoscale*, 2016, **8**, 17639–17644.
16 G. Martínez-Guajardo, A. P. Sergeeva, A. I. Boldyrev, T. Heine, J. M. Ugalde and G. Merino, *Chem. Commun.*, 2011, **47**, 6242–6244.
17 J. Zhang, A. P. Sergeeva, M. Sparta and A. N. Alexandrova, *Angew. Chem., Int. Ed.*, 2012, **51**, 8512–8515.
18 M. R. Fagiani, X. Song, P. Petkov, S. Debnath, S. Gewinner, W. Schöllkopf, T. Heine, A. Fielicke and K. R. Asmis, *Angew. Chem., Int. Ed.*, 2017, **56**, 501–504.
19 Y.-J. Wang, X.-R. You, Q. Chen, L.-Y. Feng, K. Wang, T. Ou, X.-Y. Zhao, H.-J. Zhai and S.-D. Li, *Phys. Chem. Chem. Phys.*, 2016, **18**, 15774–15782.
20 W. Huang, A. P. Sergeeva, H.-J. Zhai, B. B. Averkiev, L.-S. Wang and A. I. Boldyrev, *Nat. Chem.*, 2010, **2**, 202–206.
21 J. O. C. Jiménez-Halla, R. Islas, T. Heine and G. Merino, *Angew. Chem., Int. Ed.*, 2010, **49**, 5668–5671.
22 J. Manz, *J. Am. Chem. Soc.*, 1980, **102**, 1801–1806.
23 T. Momose, H. Hoshina, M. Fushitani and H. Katsuki, *Vib. Spectrosc.*, 2004, **34**, 95–108.
24 M. E. Fajardo, *J. Phys. Chem. A*, 2013, **117**, 13504–13512.
25 D. Yu. Zubarev and A. I. Boldyrev, *Phys. Chem. Chem. Phys.*, 2008, **10**, 5207.

26 A. P. Sergeeva, I. A. Popov, Z. A. Piazza, W.-L. Li, C. Romanescu, L.-S. Wang and A. I. Boldyrev, *Acc. Chem. Res.*, 2014, **47**, 1349–1358.
27 W.-L. Li, Y.-F. Zhao, H.-S. Hu, J. Li and L.-S. Wang, *Angew. Chem., Int. Ed.*, 2014, **53**, 5540.
28 A. I. Boldyrev and L.-S. Wang, *Phys. Chem. Chem. Phys.*, 2016, **18**, 11589–11605.
29 L.-S. Wang, *Int. Rev. Phys. Chem.*, 2016, **35**, 69–142.
30 N. G. Szwacki, A. Sadrzadeh and B. I. Yakobson, *Phys. Rev. Lett.*, 2007, **98**, 166804.
31 H.-J. Zhai, *et al.*, *Nat. Chem.*, 2014, **6**, 727–731; G. Martínez-Guajardo, J. L. Cabellos, A. Díaz-Celaya, S. Pan, R. Islas, P. K. Chattaraj, T. Heine and G. Merino, *Sci. Rep.*, 2015, **5**, 11287.
32 A. J. Mannix, *et al.*, *Science*, 2015, **350**, 1513–1516.
33 Z. Zhang, E. S. Penev and B. I. Yakobson, *Nat. Chem.*, 2016, **8**, 525–527.
34 B. I. Yakobson, C. J. Brabec and J. Bernholc, *Phys. Rev. Lett.*, 1996, **76**, 2511.
35 H. Kroto, *Angew. Chem., Int. Ed. Engl.*, 1997, **36**, 1578–1593.
36 A. K. Geim, *Rev. Mod. Phys.*, 2011, **83**, 851–862.
37 T. Seideman, *Phys. Rev. Lett.*, 1999, **83**, 4971.
38 C. Romanescu, T. R. Galeev, W.-L. Li, A. I. Boldyrev and L.-S. Wang, *Angew. Chem., Int. Ed.*, 2011, **50**, 9334–9337; D. Moreno, S. Pan, L. L. Zeonjuk, R. Islas, E. Osorio, G. Martínez-Guajardo, P. K. Chattaraj, T. Heine and G. Merino, *Chem. Commun.*, 2014, **50**, 8140–8143.

